DOI 10.1007/s11141-018-9860-0
Radiophysics and Quantum Electronics, Vol. 60, No. 12, May, 2018
(Russian Original Vol. 60, No. 12, December, 2017)

RESONANCE INTERACTION OF RELATIVISTIC ELECTRONS WITH ION-CYCLOTRON WAVES. I. SPECIFIC FEATURES OF THE NONLINEAR INTERACTION REGIMES

V. S. Grach[1*] **and A. G. Demekhov**[1,2]

UDC 550.385.41+533.9

We analyze the resonant interaction of relativistic electrons with ion-cyclotron waves in the Earth radiation belts. Finite-length wave packets with variable frequencies and different amplitude profiles are considered. Specific features of the nonlinear interaction regimes are analyzed on the basis of solving numerically a system of equations of the particle motion along with the efficiency of this interaction for a single pass of the particle through the wave packet. In the first part of this work, the peculiarities of the trajectories of individual particles are analyzed. The influence of the shape of the wave packet on the well-known regimes, such as particle trapping by the wave field and particle phase bunching, which leads to a non-zero average variation in the pitch angle in an inhomogeneous medium, are considered. It is shown that a long stay of a particle near the separatrix on the phase plane in the region far from the saddle leads to a strong decrease in the pitch angle of the particle in the absence of the trapping as well. This nonlinear regime (directed scattering) is possible for comparatively low initial pitch angles. In this case, the value of the pitch angle decrease depends on the initial phase of the particle. It is shown that the trajectories corresponding to the directed scattering can be regarded as a transitional type of trajectories, between the trajectories of the untrapped and trapped particles. Quantitative estimates of variations in the pitch angle are obtained, and it is confirmed that the directed scattering and trapping of particles by the wave field can lead to electron precipitation into the loss cone.

1. INTRODUCTION

Electromagnetic ion-cyclotron waves (ICWs or EMIC waves) are one of the main types of plasma oscillations in the Earth's magnetosphere. They are observed in a wide range of the McIlwaine parameters and longitudes, $L = 3$–10 and 5 through 21 hours of the magnetic local time, respectively [1–5]. In quiet times, the maximum of ICW activity occurs at high L-shells ($L > 6$) and the daytime sector of the magnetosphere, i.e., from 9 to 15 hours of the magnetic local time [1, 4, 5]. During perturbations, ICWs are observed at lower L-shells [4, 6].

Along with the noise ICW bursts, quasimonochromatic wave packets of the pearl or hydromagnetic chorus types with frequencies of about 1–2 Hz are detected [7–11]. According to the current concepts [7,8,12], the pearl-type emissions, i.e., periodic sequences of quasimonochromatic wave packets having periods of about 100 s and increasing frequencies within each wave packet, are excited in the regime of spike-mode generation in the Alfvén maser. A great role in the formation of the spectrum of such waves is played by the selective and nonlinear character of reflections from the ionosphere, modulation of the growth rate of the cyclotron instability by oscillations of the geomagnetic field, and reflection from the regions of gyroresonance

* vsgrach@appl.sci-nnov.ru

[1] Institute of Applied Physics of the Russian Academy of Sciences, Nizhny Novgorod; [2] Polar Geophysical Institute, Apatity, Russia. Translated from Izvestiya Vysshikh Uchebnykh Zavedenii, Radiofizika, Vol. 60, No. 12, pp. 1052–1071, December 2017. Original article submitted September 21, 2017; accepted December 28, 2017.

of heavy ions [8]. In terms of their structure, hydromagnetic chorus events or similar triggered EMIC signals [11] are similar to chorus emissions in the range of very low frequencies (VLF) in the whistler mode [13]. Probably, their generation mechanism is similar to that of VLF chorus events [14], i.e., the backward-wave oscillator regime in the magnetosphere maser [15]. The nonlinear theory of hydromagnetic-chorus generation was also developed in [16,17].

Observations show that ICW propagation is aligned with the magnetic field mainly, and the amplitudes of the waves can reach 1–7 nT [9,10,18,19]. Scattering in the loss cone caused by resonance interaction with ICWs is regarded as the main mechanism of precipitation of relativistic electrons from the radiation belts to the Earth's atmosphere [20]. This interaction was studied within the framework of the quasilinear theory [21,22], as well as allowing for the nonlinear effects, both for the monohochromatic wave [23–26] and for the wave packets having a finite length [27–29].

The authors of [23] studied the influence of phase bunching of particles and particle trapping by the wave field [30–32] on the efficiency of the scattering into the loss cone . In [26], the probability of particle trapping by the wave field and stability of the motion in this regime were estimated. It was shown in [27,28] that the scattering into the loss cone after a single pass of an electron through a variable-frequency wave packet is more efficient than that for constant-frequency wave packets. In [29], long-term interaction of electrons with the wave packet during many bounce oscillations was calculated, and the efficiency of electron precipitation was analyzed for four model wave packets having variable amplitudes. The authors of [29] also found the regime with an abnormally great drop in the pitch angle for untrapped particles (in what follows, we will call it directed scattering), which is connected, in their opinion, with the influence of the Lorentz force, i.e., its projection on the direction aligned with the radius of the Larmore circle, in the absence or particle trapping or after the particle exit from the trapping regime.

Allowing for the results obtained in [27–29], a comprehensive study of possible nonlinear regimes of the interaction of relativistic electrons with a finite-length ICW packet (numerical calculations and their physical interpretation) is still of great interest, since the dynamics of these regimes depending on the electron energy and the properties of the wave packet should be understood more thoroughly.

In this work, we use numerical calculations as a basis to consider the influence of the wave amplitude profile on the resonance interaction of relativistic electrons with a finite-length ICW packet having a variable frequency and study various nonlinear interaction regimes and efficiency of electron scattering in the case of a single pass through the wave packet. In the first part of the work presented here, specific features of the trajectories of individual particles are analyzed for three main nonlinear interaction regimes, specifically (directed scattering, a weak increase in the pitch angle for a greater fraction of untrapped particles due to their phase bunching, and particle trapping by the wave field. In the second part of the work, we will consider the dynamics of the interaction regimes and efficiency of electron scattering into the loss cone depending on the electron energy, spatial position of the wave packet, and the profile of the wave amplitude.

2. PROBLEM STATEMENT AND MAIN EQUATIONS

Consider the interaction of relativistic electrons with a packet of ion-cyclotron waves, which propagates along the magnetic field of the Earth, $\mathbf{B}_0$. Since the frequency ω of the ion-cyclotron wave is much lower than the nonrelativistic gyrofrequency of electrons, Ω_c, the resonance interaction is possible only for the relativistic particles ($\gamma > 1$) at the anomalous Doppler effect:

$$\omega - kv_{||} = -|l|\Omega_c/\gamma. \tag{1}$$

Here, $k = |k|$, $\mathbf{k}||\mathbf{B}_0$ is the wave vector, l is the resonance number (for longitudinal propagation, it is possible only at $l = 1$), $v_{||}$ is the longitudinal electron velocity (relative to the field $\mathbf{B}_0$) $\gamma = \sqrt{1 + [p/(mc)]^2}$ is the relativistic factor, m and p are the rest mass and momentum of electron, respectively, and c is the speed of light.

Under conditions where the inhomogeneity of the magnetic field $\mathbf{B}_0$ can be assumed smooth, the

amplitude of the wave $\mathbf{B}_\mathrm{w}$ is sufficiently low ($B_\mathrm{w} \ll B_0$), and the wave parameters change with time t slowly compared with Ω_c^{-1}, the system of equations, which describe the resonance interaction of a relativistic electron with an ion-cyclotron wave, can be written as

$$\frac{\mathrm{d}W}{\mathrm{d}t} = -ev_\perp |E_\mathrm{w}| \sin\Psi, \tag{2}$$

$$\frac{\mathrm{d}I_\perp}{\mathrm{d}t} = -\frac{2e}{mB_0} p_\perp (1 - n_{||}\beta_{||}) |E_\mathrm{w}| \sin\Psi, \tag{3}$$

$$\frac{\mathrm{d}\Psi}{\mathrm{d}t} = -\Delta - \frac{e}{p_\perp}(1 - n_{||}\beta_{||}) |E_\mathrm{w}| \cos\Psi, \tag{4}$$

$$\frac{\mathrm{d}z}{\mathrm{d}t} = \frac{p_{||}}{m\gamma}. \tag{5}$$

Here, the coordinate z is aligned with $\mathbf{B}_0$, $e > 0$ is the elementary charge, $p_\perp$ and $p_{||}$ the transverse and longitudinal (with respect to the field $\mathbf{B}_0$) electron momenta, respectively, E_w is the absolute value of the electric field of the wave, $n_{||} = kc/\omega$, Ψ is the angle between the vector $\mathbf{p}_\perp$ of the transverse momentum and the vector $-\mathbf{B}_\mathrm{w}$, $\beta_{||} = v_{||}/c$, $v_\perp$ is the absolute value of the transverse electron velocity, $W = (\gamma - 1)\, mc^2$ and $I_\perp = p_\perp^2/(mB_0)$ are the kinetic energy and the first adiabatic invariant of the electron, respectively, and $\Delta = \omega - kv_{||} + \Omega_\mathrm{c}/\gamma$ is the mismatch from resonance. The first term on the right-hand side of Eq. (4) is responsible for the so-called inertial, or kinematic, bunching, whereas the second term connected with the projection of the Lorentz force on the direction of the radius of the Larmor circle is responsible for the force bunching.

The equatorial electron pitch angle Θ_L is expressed in terms of the energy and the adiabatic invariant by the formula

$$\Theta_L = \arcsin\sqrt{\widetilde{I}_\perp/(\gamma^2 - 1)}, \tag{6}$$

where $\widetilde{I}_\perp = I_\perp B_0/(mc^2)$. It is known [12], that at the frequency of the wave being much lower than the gyrofrequency of the particle, the energy variation rate is much lower than the variation rate of the adiabatic invariant:

$$\frac{\mathrm{d}\widetilde{W}/\mathrm{d}t}{\mathrm{d}\widetilde{I}_\perp/\mathrm{d}t} \approx \frac{\omega}{2\Omega_\mathrm{c}} \ll 1, \tag{7}$$

where $\widetilde{W} = \gamma - 1$. Thus, one can assume that under resonant interaction of electron with ICWs, the variation in the pitch angle Θ_L is determined completely by the variation in the value of $I_\perp$.

Many works deal with an analytical study of the resonance interaction of a charged particle with a wave (including an ion-cyclotron wave), e.g., [23, 26, 30–33], et al. The motion of the particles can be approximately described by equations of the nonlinear-pendulum type [30]. In this case, the second term in Eq. (4) is usually neglected. In the presence of the minimum of the effective potential, the particle can be trapped by the wave field. The trapped particles move along finite trajectories, which correspond to oscillations in the potential well. The trajectories of the untrapped particles are infinite.

The dimensionless parameter of the effective inhomogeneity can be written in the form $\mathcal{R} = \sigma_R R$, where the term $\sigma_R = \pm 1$ determines the sign of the efficient inhomogeneity, and

$$R = \frac{|\mathrm{d}\Delta/\mathrm{d}t|}{\Omega_\mathrm{tr}^2}. \tag{8}$$

Here, Ω_tr^2 is the squared frequency of electron oscillations in the wave field near the minimum of the effective wave potential [33]:

$$\Omega_\mathrm{tr}^2 = (1 - n_{||}^{-2}) \frac{ek_{||}^2 v_\perp |E_\mathrm{w}|}{m\omega\gamma} = (1 - n_{||}^{-2}) \frac{e\omega n_{||}^2 v_\perp |E_\mathrm{w}|}{mc^2\gamma}. \tag{9}$$

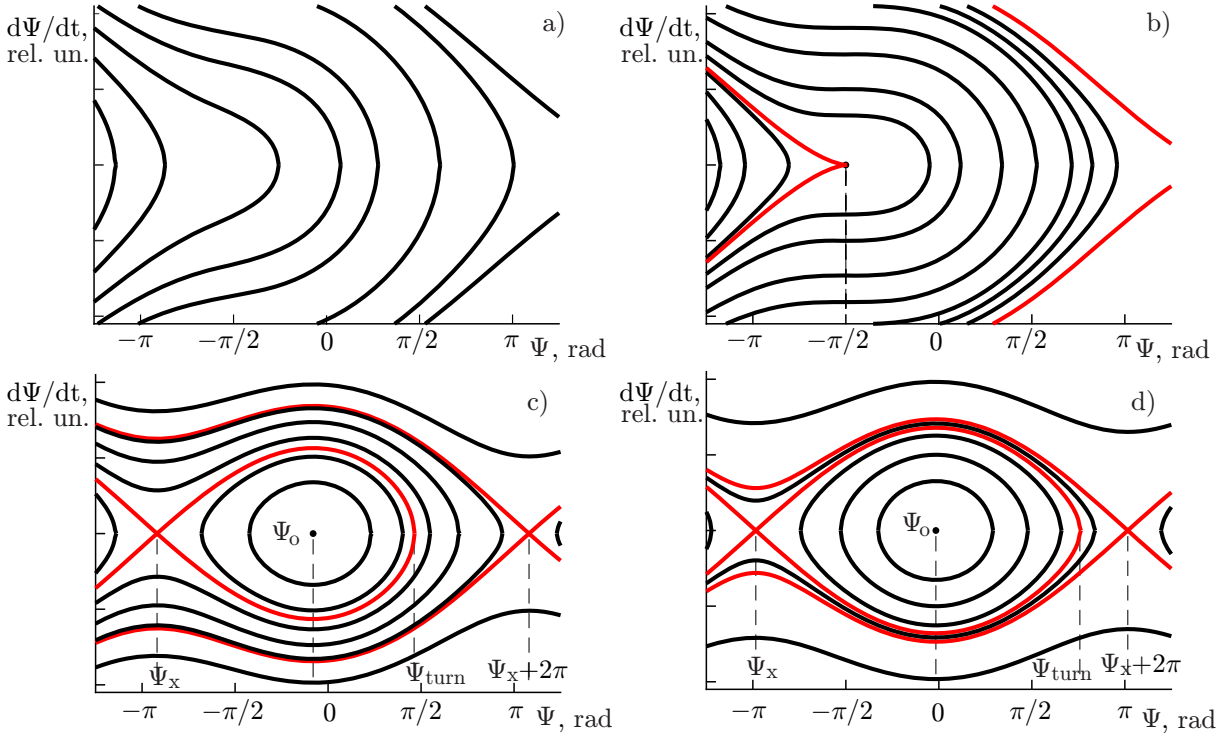

Fig. 1. Schematic phase portrait of the considered system on the plane $(\Psi, \mathrm{d}\Psi/\mathrm{d}t)$ for $R^0 = 1.25$, $R^0 = 1.00$, $R^0 = 0.25$, and $R^0 = 0.05$ (*a*, *b*, *c*, and *d*, respectively). The separatrices are shown in the red color.

The minimum of the effective potential exists only at $R < 1$. Correspondingly, the particle can be trapped by the wave field also at $R < 1$. In the case, where $R \gg 1$, the particle motion can be assumed to be linear: the particle is untrapped, and the phase at the resonance point Ψ_{res} is determined by the unperturbed trajectory and depends linearly on the initial phase. The total variation in the pitch angle (and energy) is determined by the initial phase, which can lead to a diffusion in $I_\perp$ (and, correspondingly, pitch angle diffusion) for the particle ensemble. At $R \ll 1$, the nonlinear regime is realized, which is characterized by phase bunching of the particles and a drift of the values of $I_\perp$, for both the untrapped particles and the particles trapped by the wave field. Schematic phase portraits for various values of R^0 on the plane $(\Psi, \mathrm{d}\Psi/\mathrm{d}t)$ [30–32] are shown in Fig. 1. Here and in what follows, the superscript 0 denotes the values calculated with respect to the unperturbed trajectory (with no allowance for the terms proportional to $|E_{\mathrm{w}}|$ in system (2)–(5)).

In the linear case ($R \gg 1$, see Fig. 1*a*; the corresponding values are labeled with the subscript "lin"), one can use the stationary-phase method [12] to estimate the variation $\Delta I_\perp^{\mathrm{lin}}$ in the value of $I_\perp$ of the untrapped particle. This method yields

$$\Delta I_\perp^{\mathrm{lin}} = I_{\perp\mathrm{end}}^{\mathrm{lin}} - I_{\perp 0} = |K_{I_\perp}^0| \sqrt{\frac{2\pi}{|\Psi_t''|_{\mathrm{res}}^0}} \sin\left[\Psi_{\mathrm{res}} + \mathrm{sgn}(\Psi_t''|_{\mathrm{res}}^0)\pi/4\right]. \tag{10}$$

Here, $\Psi_t'' = \mathrm{d}^2\Psi/\mathrm{d}t^2$, the subscript "res" denotes the values calculated at the resonance point, $K_{I_\perp} \equiv -2ep_\perp(1 - n_{||}\beta_{||})|E_{\mathrm{w}}|/(mB_0)$ is the coefficient in front of the term $\sin\Psi$ on the right-hand side of Eq. (3), and $I_{\perp 0}$ and $I_{\perp\mathrm{end}}$ are the first adiabatic invariant of the electron before and after trapping, respectively. The complete variation in the pitch angle can be expressed in terms of $\Delta I_\perp^{\mathrm{lin}}$ (allowing for $\gamma \approx \mathrm{const}$):

$$\Delta\Theta_L^{\mathrm{lin}} = \arcsin\left[\sqrt{\frac{|K_{I_\perp}^0|\sqrt{2\pi/|\Psi_t''|_{\mathrm{res}}^0}\sin(\Psi_{\mathrm{res}} \pm \pi/4) + I_{\perp 0}}{\gamma^2 - 1}}\right] - \Theta_{L0}, \tag{11}$$

where the subscript 0 corresponds to the initial value.

Schematic phase portraits for the nonlinear case (the NL superscript, $R \ll 1$) are shown in Fig. 1*c* and Fig. 1*d*. When the allowance for the inhomogeneity is more accurate, the size and position of the separatrix vary in the phase space $(I_\perp, \Psi, \mathrm{d}\Psi/\mathrm{d}t)$. As the particles approach the separatrix, most of them go round it on the external side and cross it in the saddle-point area at the resonance moment [23, 31, 32]. The total variation in the adiabatic invariant for such untrapped particles (between the moments at which the particle stays far from the separatrix before and after the interaction) can be estimated as follows: [23, 31, 32]:

$$\Delta I_\perp^{\mathrm{NL}} = I_{\perp\mathrm{end}}^{\mathrm{NL}} - I_{\perp 0} = \pm\frac{8}{\pi}\frac{|K_{I_\perp}^0|}{\Omega_{\mathrm{tr}}}. \tag{12}$$

In this case, the total variation in the value $I_\perp$ (and, correspondingly, the angle Θ_L) does not depend on the initial phase, and the resonance phase of the untrapped particles can take values in a narrow range

$$\Psi_{\mathrm{turn}} < \Psi_{\mathrm{res}} < \Psi_{\mathrm{x}} + 2\pi, \tag{13}$$

where the value Ψ_{x} corresponds to the saddle of the separatrix in the phase plane $(\Psi, \mathrm{d}\Psi/\mathrm{d}t)$, and $\sin\Psi_{\mathrm{x}} = \pm R^0$, Ψ_{turn} is the opposite point of the separatrix (the turning point), for which the condition $\mathrm{d}\Psi/\mathrm{d}t = 0$ is also fulfilled. At $R^0 \to 1$, the phases corresponding to the saddle, the state of equilibrium and the turning point coincide ($\Psi_{\mathrm{x}} \approx \Psi_{\mathrm{o}} \approx \Psi_{\mathrm{turn}}$) and the resonance phase of the transit-type particle can be arbitrary (see Fig. 1*b*). At $R^0 \to 0$, we have $\Psi_{\mathrm{x}} \approx -\pi$, $\Psi_{\mathrm{turn}} \approx \pi$ and, according to (13), the resonance phase of the untrapped particles is approximately equal to $\Psi_{\mathrm{res}} \approx \pi$ (see Fig. 1*d*).

The sign of the parameter $\Delta I_\perp^{\mathrm{NL}}$ and the phases $\Psi_{\mathrm{x}}, \Psi_{\mathrm{o}}$ and Ψ_{turn} are determined by the sign of the effective inhomogeneity σ_R, the wave mode, and the resonance type [32]. We consider the interaction of an electron with an ICW under the anomalous Doppler effect (1) for the case of wave packet propagation away from the magnetic equator, which corresponds to the assumption about generation of this package in the equatorial region. In this case, especially allowing for the positive drift of the frequency in the package, $\sigma_R < 0$, so we have $\Delta I_\perp^{\mathrm{NL}} > 0$, $\Psi_{\mathrm{x}} = \arcsin(R^0) - \pi$, $\Psi_{\mathrm{o}} = -\arcsin(R^0)$, and $\cos\Psi_{\mathrm{turn}} - R^0\Psi_{\mathrm{turn}} = \cos\Psi_{\mathrm{x}} - R^0\Psi_{\mathrm{x}}$.

Thus, in this case the nonlinear regime for untrapped particles can lead to an average increase in the pitch angle. It is evident that estimate (12) is applicable only in the case, where the transverse kinetic energy, which is calculated through the use of it, does not exceed the total energy, i.e., when the inequality $p_{||}^2 \geq 0$ is fulfilled, or

$$I_{\perp\mathrm{end}} < (\gamma^2 - 1)mc^2. \tag{14}$$

In accordance with [23, 31, 32], this nonlinear effect, specifically, the increase in the pitch angle by an approximately identical value for a significant fraction of untrapped particles to the phase grouping in the saddle region, will be termed phase bunching hereafter.

A certain part of the particles at $R \ll 1$ can be trapped. The trapped particles oscillate inside the separatrix, which, allowing for the motion of the separatrix on the plane $(\Psi, I_\perp)$, can lead to a strong decrease in $I_\perp$ [32] in the case under consideration. In what follows, it will be shown that the effect of the significant decrease in the pitch angle takes place also for the untrapped particles propagating near the separatrix and far from the saddle (at $R \lesssim 1$).

In the general case, the signs of the variations in the pitch angle of the trapped particles and the main part of the untrapped particles are determined by the sign of the effective inhomogeneity σ_R. Thus, when whistler-mode waves interact with electrons at the fundamental cyclotron resonance, an increase in the frequency leads to acceleration of the trapped particles by waves [33, 34], and the initial energy of the waves can be insufficient for this acceleration. The required energy goes into the waves from the untrapped particles, whose bunching determines the decrease in their energy [35]. The interaction of relativistic electrons with ICWs does not lead to a significant energy exchange between particles and waves, therefore, the approximation of the given amplitude of the wave package is justified.

3. NUMERICAL CALCULATIONS

For the interaction of test particles with given initial conditions and an ICW packet having a finite length, system (2)–(5) was solved numerically by the third-order Runge—Kutta method. A single transit of the electron through the packet was calculated with allowance for the anomalous cyclotron resonance. Since the velocity of wave packet propagation is much lower than the electron velocity, the motion and evolution of the packet are insignificant, although they are allowed for in the equations.

3.1. Parameters of the plasma and the wave packet. Preliminary analysis

The plasma parameters chosen for the calculations correspond to [27], specifically, we consider wave packets having frequencies, which increase with time (of the hydromagnetic-chorus type) in a frequency range lower than the gyrofrequency $\Omega_{\rm H}$ of protons, but higher than the gyrofrequency of helium ions He^+ at the L-shell $L = 5.5$ under the electron density $N_{\rm e} = 178$ cm^{-3}. The ion composition is as follows: ions of hydrogen ($N_{\rm H^+} = 0.81N_{\rm e}$), helium ($N_{\rm He^+} = 0.095N_{\rm e}$), and oxygen ($N_{\rm O^+} = 0.095N_{\rm e}$) are present. A noticeable fraction of helium in the plasma is required to ensure that the resonance electron energies are relatively low (about 1–3 MeV). The geomagnetic field B_0 is calculated within the dipole approximation.

We considered a wave packet having the length $L_{\rm pt} = 7000$ km and a linear frequency drift (the packet frequency decreases linearly from the trailing edge $z = z_1$ towards the leading edge $z = z_2$ in the range from $\omega = 0.76\Omega_H = 2.3$ Hz to $\omega = 0.46\Omega_H = 1.4$ Hz). The calculations were performed for two variants of the packet shape, specifically, one with a constant amplitude of the electric field $E_{\rm w}$ (rectangular packet) and the other, with the amplitude distributed by the Gauss law (Gaussian package), and the following three variants of the position of the trailing edge of the package: $z_1^{(1)} = -10c/\Omega_H = -90$ km (almost the equator, packet 1), $z_1^{(2)} = z_1^{(1)} + L_{\rm pt}/4$ (packet 2), and $z_1^{(3)} = z_1^{(1)} + L_{\rm pt}/2$ (packet 3). The positive direction of the z axis corresponds to the direction of wave propagation and the motion of resonance electrons. For the third packet, the leading edge borders on the zone of cyclotron resonance of the He^+ ions. Correspondingly, the positions of the wave packet being farther from the equator were not considered, since in this case, it was necessary to allow for the influence of cyclotron wave absorption on the shape of the wave packet. The maximum value of the wave magnetic field is equal to $B_{\rm w} = 2.2$ nT (the values of the maximum electric field $E_{\rm w}$ for different packet positions are not identical). This set of the packet parameters corresponds to the characteristics of the waves observed in a real event [19].

The following range of the initial parameters is considered for the electrons: $W_0 = 0.98$–2.2 MeV and $\Theta_{L0} = 30°$–$70°$. They were chosen keeping in mind that it is necessary to ensure efficiency of interaction of the particles with the specified packets in the plasma with the chosen parameters.

The calculations were performed for 8 values of the initial energy in the specified range, 41 values of the initial pitch angle (with a step of 1°) and 360 values of the initial phase, which were distributed evenly within the range $[0, 2\pi]$.

Figure 2 shows the position of the resonance point $z_{\rm res}^0$ (the coordinate z is normalized to the Earth radius) and the inhomogeneity parameter R^0 (8) at this point as functions of the initial values of the pitch angle at the equator Θ_{L0} and electron energy W_0, which were calculated for the unperturbed trajectory. It is seen in this figure that the position of the resonance point shifts towards the equator (the point of entry into the package) as the initial pitch angle increases and the energy decreases. At sufficiently high pitch angles ($\Theta_{L0} > \Theta_{L*}$), the resonance condition is not fulfilled in the region of the wave packet (the value Θ_{L*} increases with increasing energy). Evidently, the change in the character of the curves depending on the initial position of the wave packet is due to a variation in the frequency inside the packet.

The parameter R^0 for the rectangular packet increases with increasing energy and decreases to the values $R^0 \le 0.1$ as the pitch angle Θ_{L0} grows up. Note that the decrease in R^0 with increasing pitch angle Θ_{L0} is connected with the increase in the value $\Omega_{\rm tr}^2$ (9), rather than the decrease in the derivative $\mathrm{d}\Delta/\mathrm{d}t$. This increase is due to the fact that the greater initial pitch angle at a constant energy is corresponded by

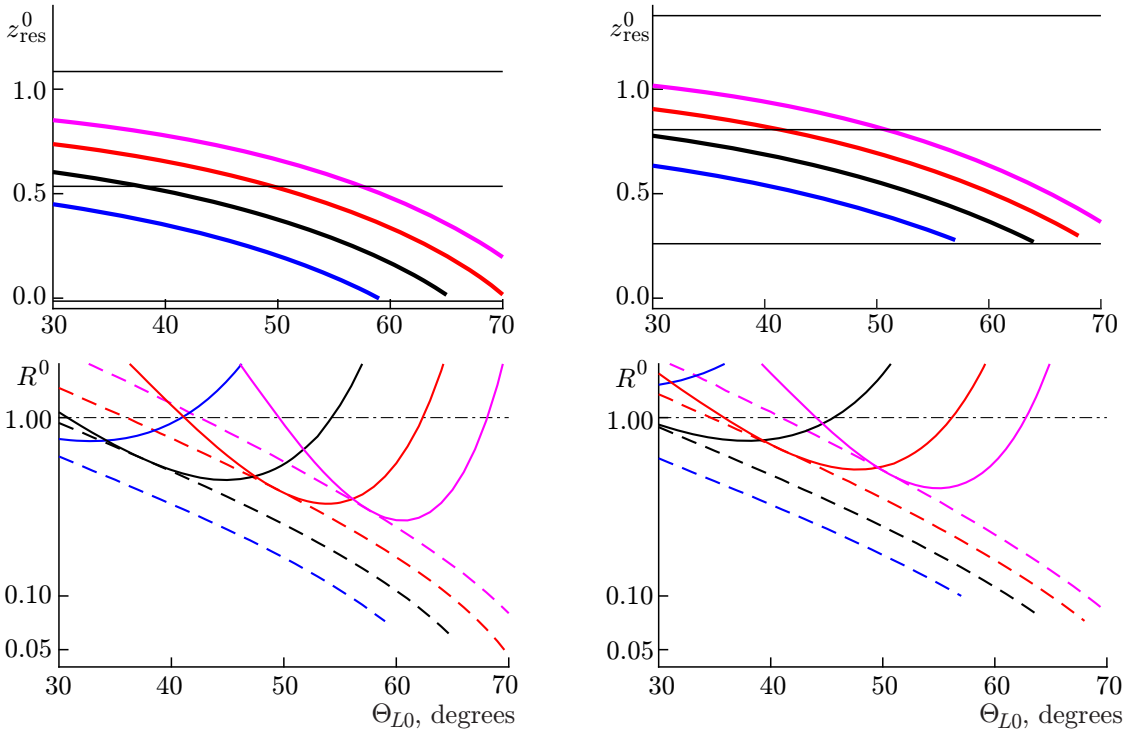

Fig. 2. Position of the resonance point and the value of the parameter R^0 at this point depending on the initial electron parameters for packets 1 and 2 (left-hand and right-hand columns, respectively). The blue, black, red, and purple line correspond to $W_0 = 0.98$, 1.30, 1.50, and 2.20 MeV, respectively. The black horizontal lines in the top panels show the boundaries and the middle of the packet. The solid lines in the bottom panels correspond to the Gaussian packet, and the dashed lines, to the rectangular packet.

a higher transverse velocity $v_\perp$ and a lower longitudinal velocity $v_{||}$ and, consequently, greater proximity of the resonance point $\Delta = 0$ to the equator (see top panels in Fig. 2), where the wave frequency is higher, and the gyrofrequency is lower, which yields a greater refractive index $n_{||}$. Qualitatively, the character of the dependence $R^0(W_0, \Theta_{L0})$ is the same as for the constant frequency packet [23].

For the Gaussian wave packet, the parameter R^0 has a minimum in the pitch angles. The value of this minimum in the considered energy range decreases as the energy increases (and has a minimum in a wider energy range). Note that even under the optimal conditions, the ratio R^0 is sufficiently great for the Gaussian packet: $R^0_{\rm min} \approx 0.4$–$0.5$. As the energy increases, the angular dependences shift towards the greater pitch angles. As the package moves away from the equator at a constant energy, the dependences $z^0_{\rm res}(W_0, \Theta_{L0})$ and $R^0(W_0, \Theta_{L0})$ shift towards the lower pitch angles, and at a constant pitch angle, towards the higher energies (but in this case, the difference in the dependences $R^0(W_0, \Theta_{L0})$ for different positions of the packages is nearly unnoticeable for the rectangular packet).

Basing on the above-said, one can naturally assume that for the Gaussian wave packet, the efficiency of electron interaction with the packet depends on the electron energy and the packet position much stronger, than that for the rectangular one. At a fixed position of the packet, the dependence of the interaction efficiency (i.e., the average variation in the pitch angle and/or number of trapped particles) shifts presumably towards the higher pitch angles as the electron energy increases. The shift of the packet away from the equator, in its turn, should lead to a shift of this dependence towards the higher energies (at a constant pitch angle) or lower pitch angles (at a constant energy).

In the first part of our paper, we will restrict our consideration to the analysis of possible interaction regimes and presentation of results for individual particles (or particle groups). In the second part, we will present the integral results for the entire ensemble of the considered test particles and analyze the dynamics of the interaction regimes depending on the electron energy and properties of the packet.

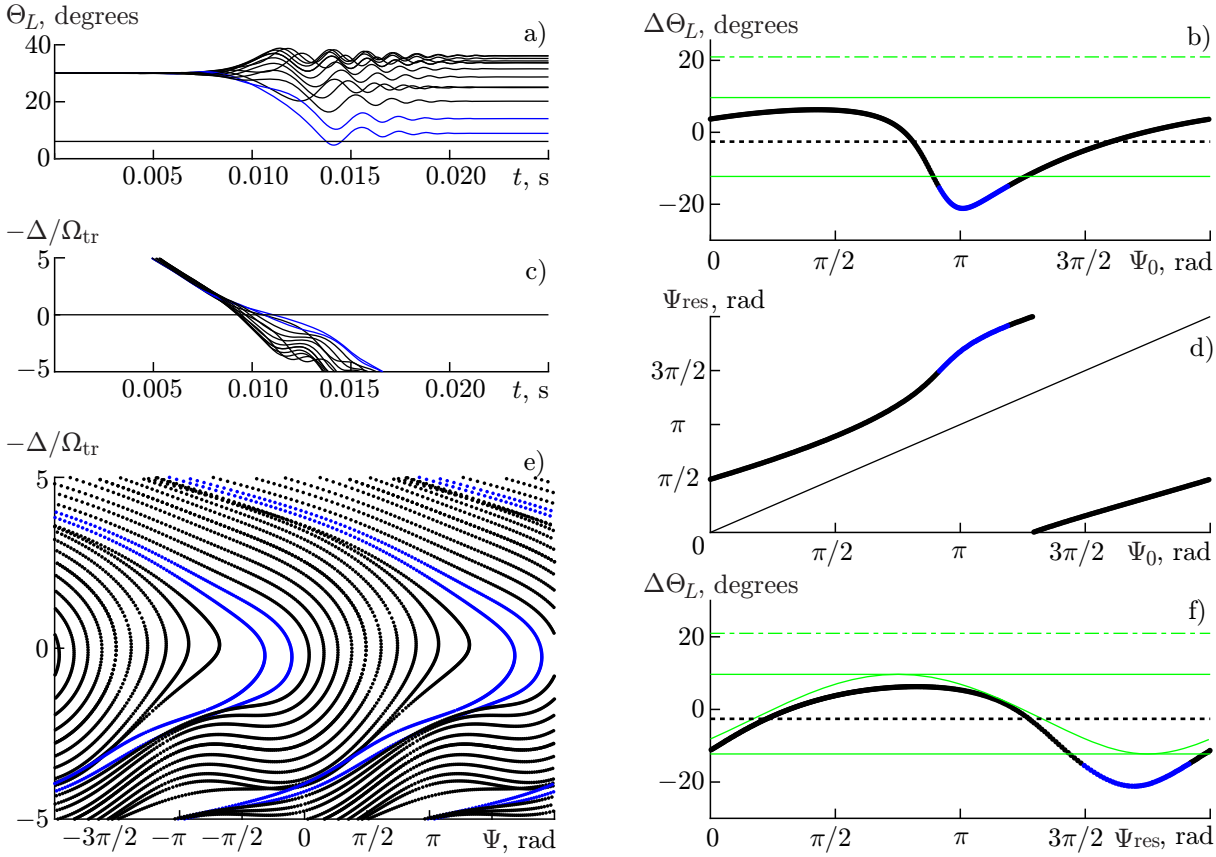

Fig. 3. Calculation results for the Gaussian wave packet (packet 2) under the conditions of weak nonlinearity at $W_0 = 0.98$ MeV, $\Theta_{L0} = 30^\circ$ and $R^0 = 1.56$. The blue and black colors correspond to the untrapped particles with $\Delta\Theta_L < -15^\circ$ and $\Delta\Theta_L \geq -15^\circ$, respectively. The horizontal line in panel *a* shows the pitch angle $\Theta_{\rm CR}$ which corresponds to the loss cone. The black dashed line in panels *b* and *e* corresponds to. the average variation $\langle\Delta\Theta_L\rangle$, the green solid lines correspond to estimate (11) (the horizontal ones, to the maximum increase and decrease), and the dash-dotted green lines, to estimate (12). The thin solid line in panel *d* corresponds to the dependence $\Psi_{\rm res} = \Psi_0$

3.2. Calculation results

Figures 3–6 present the results of calculations for the Gaussian packet (packet 2) with four combinations of the parameters W_0 and Θ_{L0} which correspond to four qualitatively different interaction regimes. We present the time dependences $\Theta_L(t)$ and $\Delta(t)$ and the trajectories on the phase plane $\Delta(\Psi)$ for 16 particles with different initial phases (for clarity, the phase trajectories are constructed in the range $-2\pi \leq \Psi \leq 2\pi$), as well as the dependences $\Delta\Theta_L(\Psi_0, \Psi_{\rm res})$ and $\Psi_0(\Psi_{\rm res})$. In the calculations, the particle is regarded formally as trapped by the wave field if the number of the points on the trajectory, at which the resonance condition $\Delta = 0$ is fulfilled exactly, exceeds unity. The resonance phase for the trapped particles is determined at the first resonance point. Note that the coefficients of the equation system under consideration depend on the time explicitly, i.e., the system is non-autonomous. Therefore, the trajectories on the phase plane may cross (different trajectories reach the same point at different time moments).

The initial values of W_0, Θ_{L0} and the unperturbed value of R^0 are shown in the figures. The values corresponding to estimates (11)–(13) are also presented. Analysis of system (2)–(5) for unperturbed trajectories (at $E_{\rm w} = 0$) shows that for the parameters of the plasma and electrons under consideration and a single transit of the packet, $(\mathrm{d}^2\Psi/\mathrm{d}t^2)|^0 < 0$, therefore, the maximum decrease in the pitch angle in estimate (11) corresponds to $\Psi_{\rm res} = 7\pi/4$.

The figures demonstrate that under the considered parameters of the wave, the region of resonant

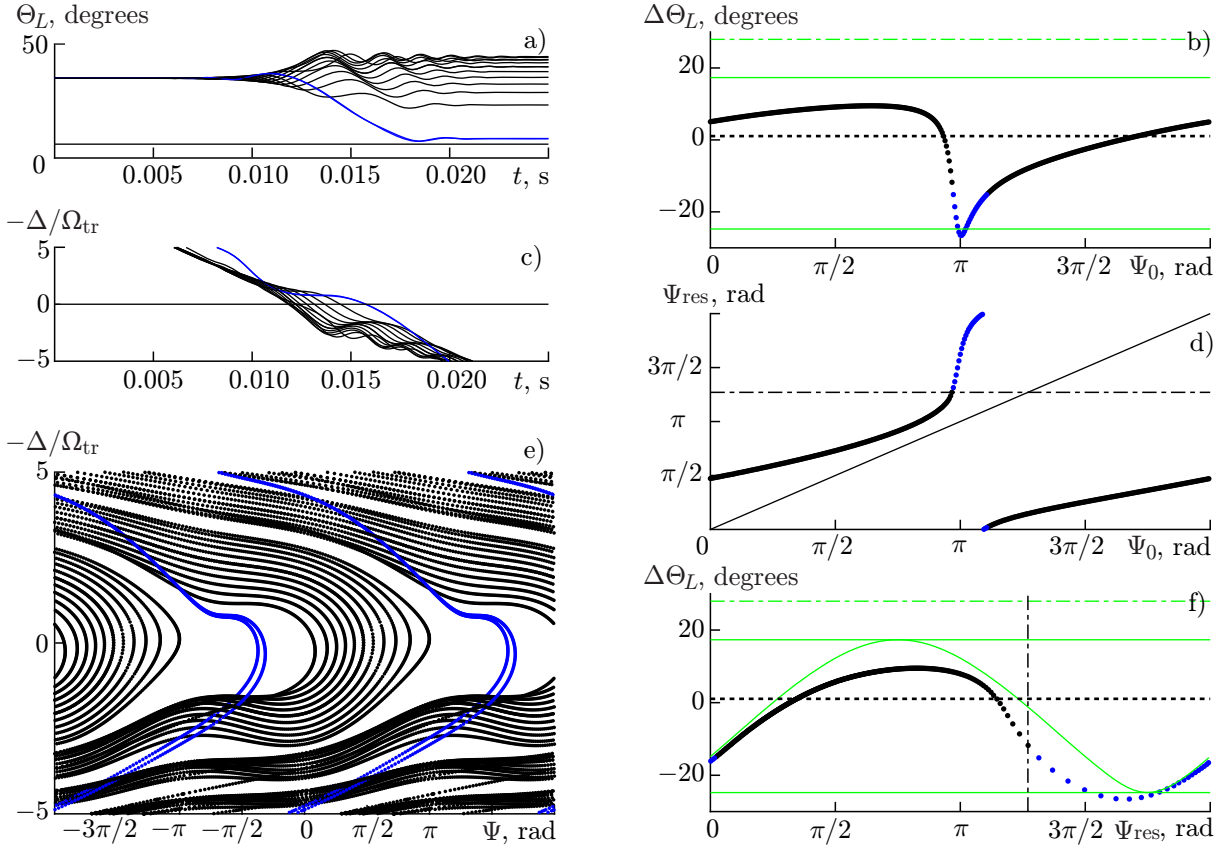

Fig. 4. Calculation results for the Gaussian wave packet (packet 2) in the presence of directed scattering and bunching of untrapped particles at $W_0 = 1.3$ MeV, $\Theta_{L0} = 35°$, and $R^0 = 0.75$. The notations are the same as in Fig. 3. The black dash-dotted lines in panels *d* and *f* correspond to the values $\Psi_{\rm x} + 2\pi$ and $\Psi_{\rm turn}$ ($\Psi_{\rm turn} \approx 0$ at a given value of R^0).

interaction of the package with the electron is determined by the effective length of the package, since it is shorter than or comparable with the size of the resonance region. Depending on the parameters W_0 and Θ_{L0}, several regimes of electron interaction with the Gaussian package are possible.

For the case shown in Fig. 3 (low pitch angle), the unperturbed value is $R^0 > 1$. There are no trapped particles in this case. The dependence $\Psi_{\rm res}(\Psi_0)$ contains both linear intervals, and a pronounced nonlinear interval, which indicates that there occurs phase bunching of particles during their transit to the resonance region. The nonlinear interval corresponds to the particles with a great variation in the pitch angle (blue curves). However, on the phase plane, these curves do not differ qualitatively from the black curves, which correspond to the "conventional" untrapped particles. The qualitative difference in these trajectories is seen in Fig. 3*c*: for them, the derivative $\mathrm{d}\Delta/\mathrm{d}t$ is smaller, i.e., the particles moving along these trajectories stay longer in the resonance region.

The dependence $\Delta\Theta_L(\Psi_{\rm res})$ is close to the sinusoidal one, the average value $\langle\Delta\Theta_L\rangle$ is little different from $\langle\Delta\Theta_L\rangle^{\rm lin}$. In the region $\Delta\Theta_L < 0$, which corresponds to the nonlinear interval of the dependence $\Psi_{\rm res}(\Psi_0)$ (blue curves), $\Delta\Theta_L < \Delta\Theta_L^{\rm lin}$, and one can see in Fig. 3*a* that there are particles for which the pitch angle $\Theta_{L\,\rm end}$ is close to the loss cone. In what follows, the nonlinear effect corresponding to the strong decrease in the pitch angle for the untrapped particles (compared with linear estimate (11) and the maximum increase) will be called directed scattering. In the region $\Delta\Theta_L > 0$ depending on $\Delta\Theta_L(\Psi_{\rm res})$, there is an extended interval ($\pi/2 < \Psi_{\rm res} < 5\pi/4$), for which $\Delta\Theta_L \approx \mathrm{const} < (\Delta\Theta_L^{\rm lin})^{\max} < \Delta\Theta_L^{\rm NL}$; this can be regarded as an indication of particle bunching.

Figure 4 shows the case with a lower value of R^0 ($R^0 < 1$), but there are no trapped particles here

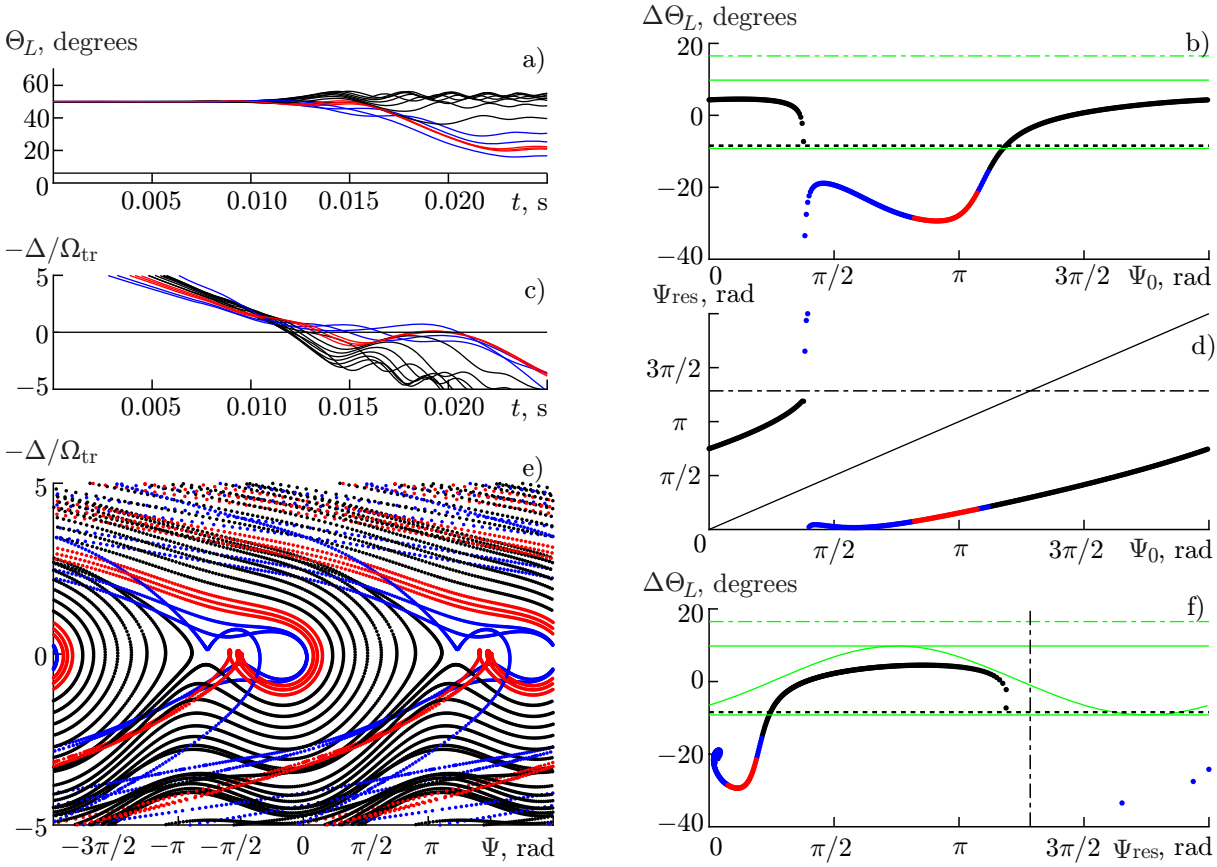

Fig. 5. Results of calculations for the Gaussian wave packet (packet 2) in the presence of the directed scattering, bunching of the untrapped particles, and trapping of a small fraction of the particles by the wave field at $W_0 = 1.5$ MeV, $\Theta_{L0} = 50°$, and $R^0 = 0.78$. The notations are the same as in Fig. 4. The red color corresponds to the trapped particles, and $\Psi_{\rm turn} \approx 0$ at a given value of R^0.

either. In this case, the dependence $\Psi_{\rm res}(\Psi_0)$ is clearly nonlinear, and the untrapped particles with great $\Delta\Theta_L$ (blue curves) correspond to a narrower region of the phase space (a narrower range of values of Ψ_0) and a sharp increase in the resonance phase $\Psi_{\rm res}$, i.e., the particles with the initial phases near π turned to be "scattered" over the resonance phases in the interval $5\pi/4 \lesssim \Psi_{\rm res} \lesssim 2\pi$. In contrast to the previous case, the blue trajectories in the phase plane differ from the black ones qualitatively. Specifically, a certain dedicated region is created, where they are located rather rarely (as compared with the black ones). In this case, a "plateau" in the dependence $\Delta(t)$ is typical of the untrapped particles with a strong variation in the pitch angles (scattered particles), i.e., the second-order resonance condition is fulfilled for them approximately:

$$\frac{{\rm d}^2\Psi}{{\rm d}t^2} \approx -\frac{{\rm d}\Delta}{{\rm d}t} \approx 0. \qquad (15)$$

Quantitatively, for these particles $\Delta\Theta_L < \Delta\Theta_L^{\rm lin}$, although in the region of the maximum pitch-angle decrease, these values are nearly coinciding. As in the case shown in Fig. 3, the maximum decrease in the pitch angle corresponds to $\Psi_{\rm res} \approx 7\pi/4$.

The bunching for the untrapped particles also takes place (the extended interval of the dependence $\Delta\Theta_L(\Psi_{\rm res})$ in the region $\Delta\Theta_L > 0$, for which $\Delta\Theta_L \approx {\rm const} < |\Delta\Theta_L^{\rm lin}|^{\rm max} < \Delta\Theta_L^{\rm NL}$).

The ensemble-average variation $\langle\Delta\Theta_L\rangle$ of the pitch angle is small in terms of its absolute value, but positive (for estimate (11) $\langle\Delta\Theta_L\rangle^{\rm lin} < 0$).

Figures 5 and 6 present the cases for high initial pitch angles ($R^0 < 1$), where many particles satisfy

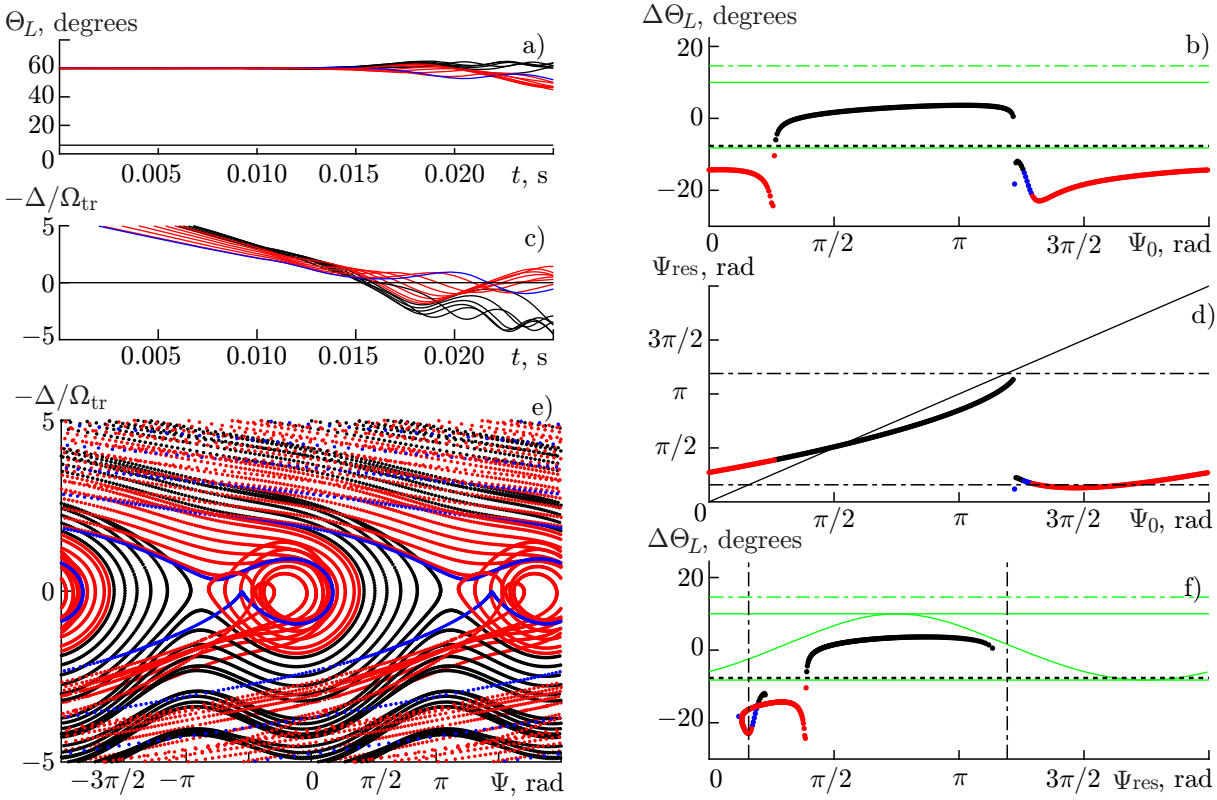

Fig. 6. Results of calculations for the Gaussian wave packet (packet 2) in the presence of the directed scattering (for a small fraction of the particles), bunching of the untrapped particles, and trapping of the particles by the wave field at $W_0 = 2.2$ MeV, $\Theta_{L0} = 60°$, and $R^0 = 0.56$. The notations are the same as in Fig. 4.

the formal condition of trapping by the wave field. In Fig. 5, the fraction of the trapped particles is not great, specifically, it is less than or comparable with the fraction of the trapped particles with a great variation in the pitch angle. Qualitatively, the blue and red trajectories have similar shapes: for both types of the trajectories, there exist sections near the resonance, where condition (15) is fulfilled. In Fig. 6, the wave traps about half of the resonant particles. In this case, a small interval of values of Ψ_0 (about $5\pi/4$) still exists, which corresponds to the untrapped particles with a strong variation in the pitch angle, for which second-order resonance condition (15) is approximately fulfilled.

The resonance phases of the untrapped particles with a great decrease in the pitch angle or, as in Fig. 4, correspond to a sharp variation in the dependence $\Psi_{\rm res}(\Psi_0)$ and stay in the vicinity of $\Psi_{\rm res} = 7\pi/4$ (several particles in Fig. 5), or have values in the vicinity of $\Psi_{\rm turn}$. In the latter case, the blue curves nearly coincide with the separatrix, which separates the trapped particles from the untrapped ones. In other words, a great decrease in the pitch angle is connected with the particle's stay near the separatrix (due to which, the time of efficient interaction of the particle and the wave increases), in the region which is the farthest from the saddle. It follows from Figs. 5*e* and 6*e* that the trapped particles also cross the separatrix at a point located far from the saddle. Quantitatively, the values of the decrease in the pitch angle for the trapped and untrapped particles (blue curves) are nearly identical. In this case, a greater part of the untrapped particles experience bunching, i.e., $0 < \Delta\Theta_L \approx \text{const} < (\Delta\Theta_L^{\rm lin})^{\max} < \Delta\Theta_L^{\rm NL}$.

Note that Figs. 3–6 present the results for various energies, since not all interaction regimes are possible for the Gaussian packet at a fixed energy (or they are not sufficiently pronounced for illustration). The dynamics of the interaction regimes depending on the electron energy and the packet position will be considered in more detail in the second part of the paper. At very low or very high pitch angles, when the resonance point is located far from the center of the packet and $R^0 \gtrsim 10$ (specific values of the pitch angles depend on the electron energy and packet position), the interaction of the electron with the package

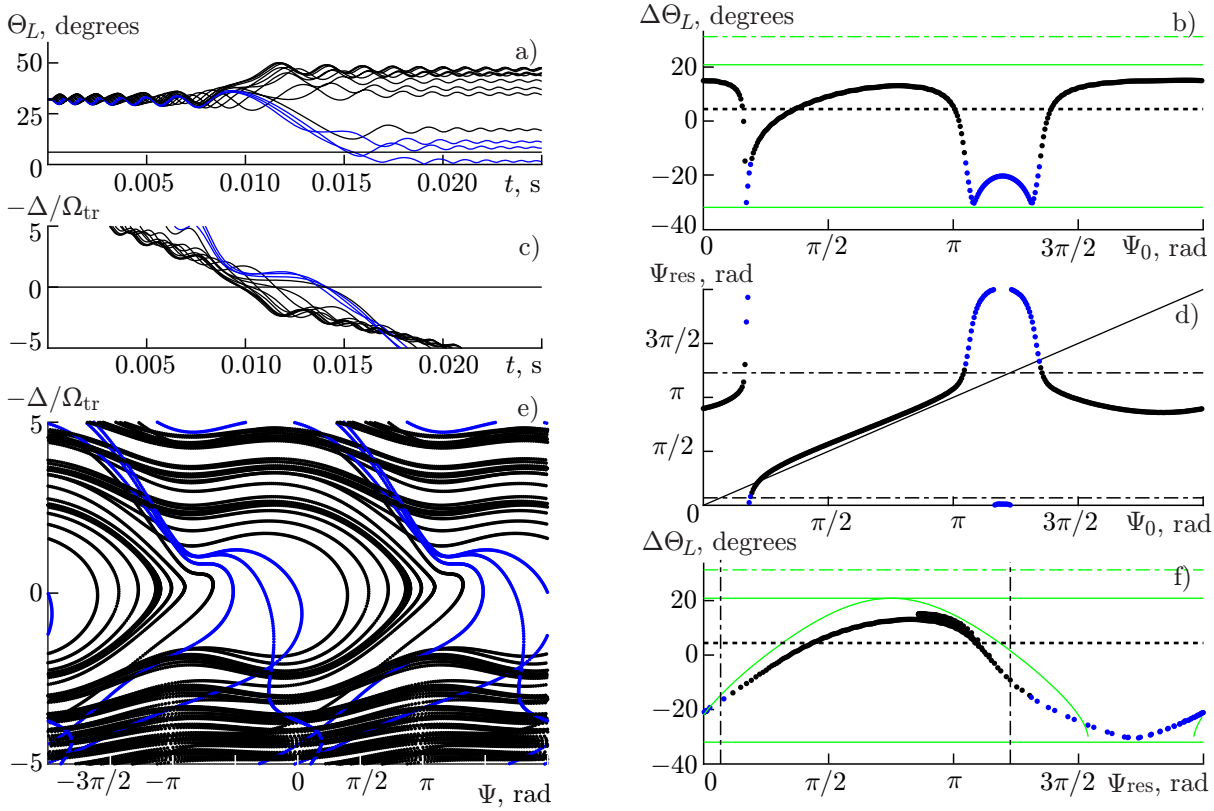

Fig. 7. Results of calculations for the rectangular package (package 2) in the presence of the directed scattering and bunching of the transit-type particles at $W_0 = 1.15$ MeV, $\Theta_{L0} = 32^\circ$, and $R^0 = 0.65$. The notations are the same as in Fig. 4.

is described comprehensively (both qualitatively and quantitatively) by linear approximation (10) and (11).

Figures 7–9 present the calculation results for the rectangular wave packet (packet 2) for $W_0 = 1.15$ MeV and three values of the initial pitch angle Θ_{L0}, which correspond to qualitatively different interaction regimes (for a rectangular packet, all possible regimes can be observed at one and the same energy value). The notations are the same as in Figs. 3–6. For all the cases that we considered, $R^0 < 1$. However, linear estimates (11) are also presented for the sake of comparison for the particles, for which inequality (14) and the inequality

$$|\Delta I_\perp^{\rm lin}| < I_{\perp 0} \tag{16}$$

corresponding to the positivity of the adiabatic invariant are fulfilled. Estimate (12) is also presented only for those particles for which inequality (14) is fulfilled.

It follows from the figures that the chosen amplitude $B_{\rm w}$ is sufficiently great, such that at low pitch angles Θ_{L0} inequality (16) is not fulfilled in the region of negative $\Delta\Theta_L$, and at low angles, it is not fulfilled in the region of positive ones. For high Θ_{L0}, nonlinear estimates (12) are also inapplicable.

At low initial pitch angles ($\Theta_{L0} < 40^\circ$, Fig. 7), the results are close to those analogous for the Gaussian packet in Fig. 3. However, for the rectangular packet the number of sharp drops in the dependence $\Psi_{\rm res}(\Psi_0)$, which correspond to the particles with a great decrease in the pitch angle, can be more than one (three, in the presented figure). This is due to the fact that the region of the resonance interaction for the rectangular package is wider than for the Gaussian one. If phase bunching of the particles occurs during one oscillation in the wave field, this can lead to the formation of a great number of phase bunches corresponding to qualitatively different intervals in the dependence $\Psi_{\rm res}(\Psi_0)$.

Consequently, the dependence $\Delta\Theta_L(\Psi_{\rm res})$ is not unambiguous, although qualitatively, the shape of this dependence is close to the sinusoidal one. The fraction of the particles, for which the bunching takes

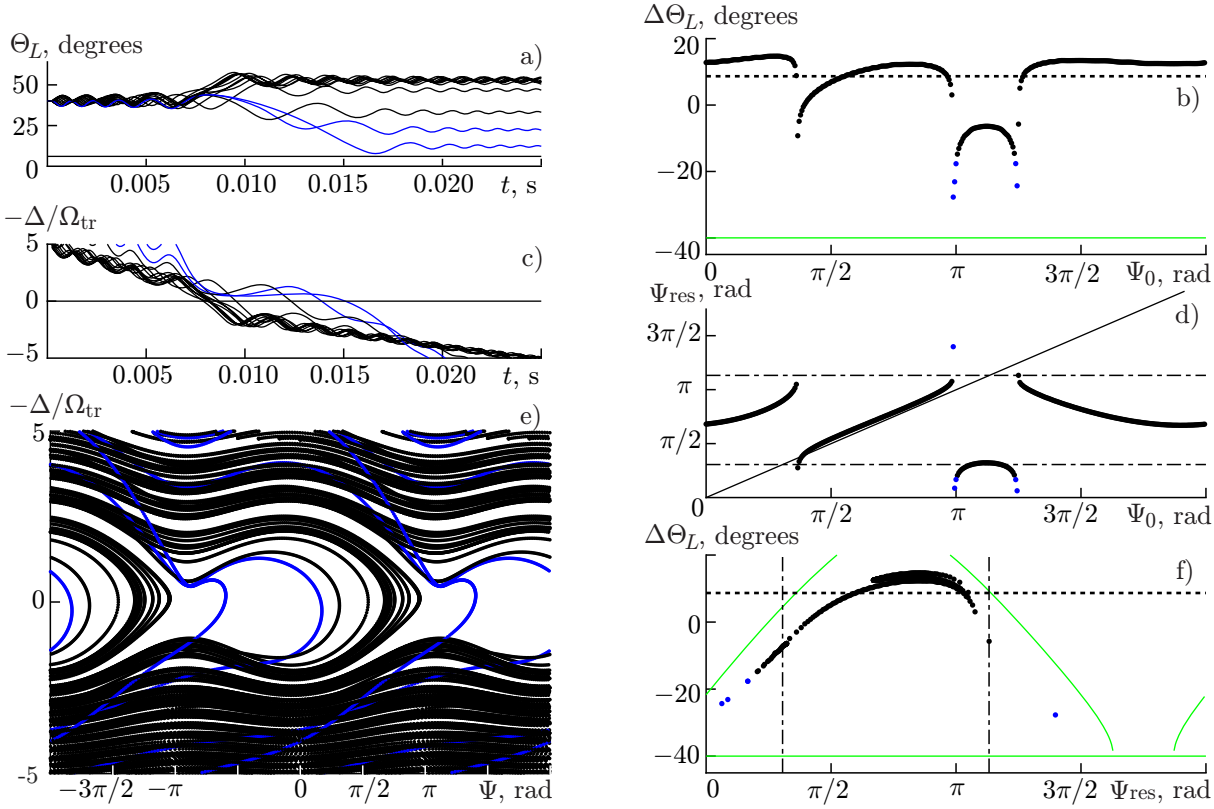

Fig. 8. Results of calculations for the rectangular package (package 2) in the presence of the directed scattering (for a small fraction of the particles) and bunching of the transit-type particles at $W_0 = 1.15$ MeV, $\Theta_{L0} = 40°$, and $R^0 = 0.4$. The notations are the same as in Fig. 4.

place ($0 < \Delta\Theta_L \approx \text{const} < (\Delta\Theta_L^{\rm lin})^{\rm max} < \Delta\Theta_L^{\rm NL}$, the resonance phases are close to the saddle point $\Psi_{\rm x}$), is comparable with the fraction of the particles, for which the directed scattering takes place, or exceeds it slightly. The average variation $\langle\Delta\Theta_L\rangle$ in the pitch angle is a small positive value in this case.

As the initial pitch angle increases (R^0 decreases), the number of phase bunches grows. Then, the fraction of the scattered particles decreases (the steepness of sharp drops in the dependence $\Psi_{\rm res}(\Psi_0)$ increases). In the case shown in Fig. 8 ($\Theta_{L0} = 40°$), the fraction of the scattered particles is less than 5%. At $\Theta_{L0} > 40°$, no untrapped particles with great variations in the pitch angle are observed. There are no trapped particles, therefore, the regions of the phase plane, which correspond to the potential wells, are not occupied by phase trajectories. Note that, as in the case of the Gaussian packet, the untrapped particles with the smallest decrease in the pitch angle have resonance phases either in the vicinity of $7\pi/4$, or in the vicinity of $\Psi_{\rm turn}$.

As the pitch angle increases further (R^0 decreases), particle trapping by the wave is possible, starting at a certain Θ_{L0} (this case is shown in Fig. 9). Since the value of R^0 is then sufficiently small, almost all of the untrapped particles are characterized by bunching, i.e., similar values of $\Delta\Theta_L > 0$ and resonance phases in interval (13). The resonance phases of the trapped particles, as in the case of the Gaussian packet, are bunched in the vicinity of $\Psi_{\rm turn}$.

When $\Theta_{L0} \geq \Theta_{L*}$, only part of the considered electrons are in resonance; in this case, all of them are trapped. If the initial pitch angle is too high (for this electron energy and packet), there are no resonance electrons (for the majority of the considered energies, this angle exceeds the highest initial pitch angle 70°). At low initial pitch angles (their specific values depend on the energy and position of the packet, more details follow in the second part of the paper), the interaction of the electron with the packet is close to the linear one.

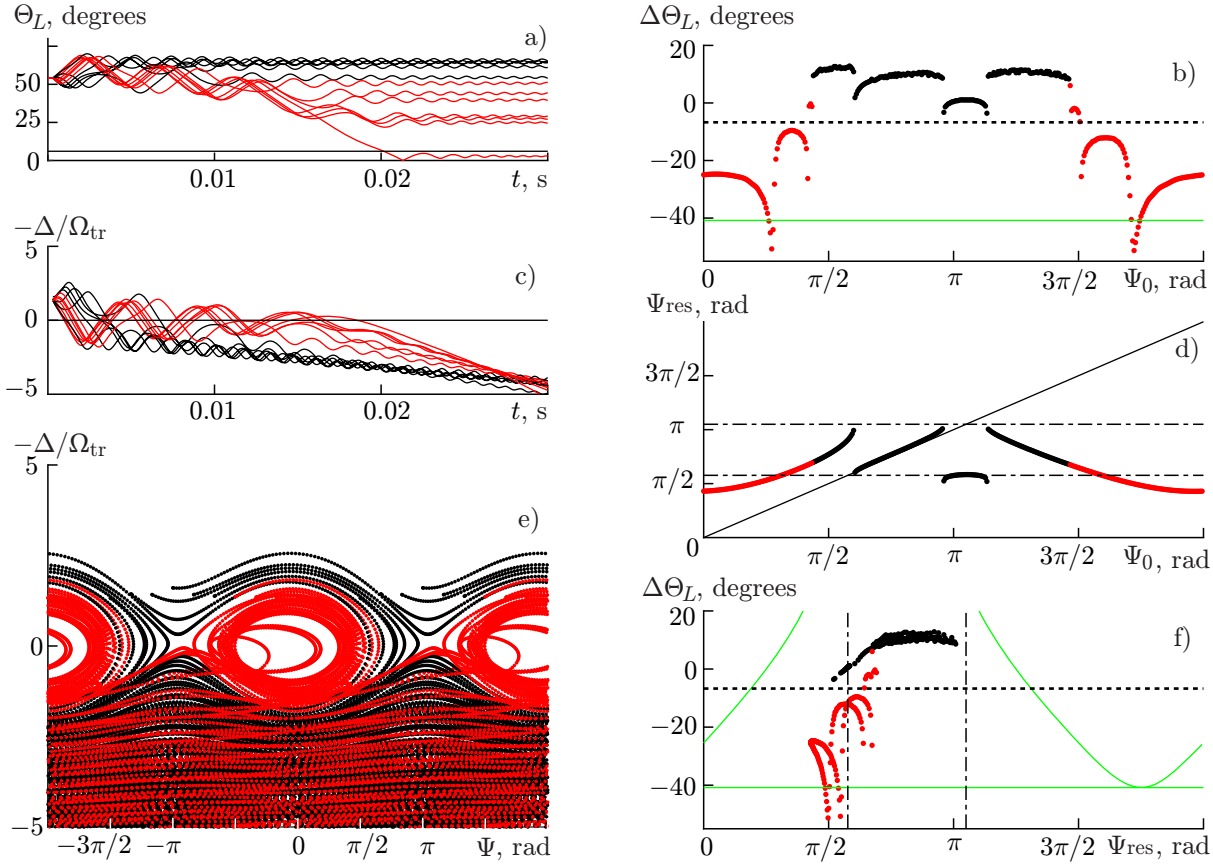

Fig. 9. Results of calculations for the rectangular wave packet (packet 2) in the presence of the bunching of the untrapped particles and trapping of the particles by the wave field at $W_0 = 1.15$ MeV, $\Theta_{L0} = 54°$, and $R^0 = 0.16$. The notations are the same as in Fig. 4.

It should be noted also that the values of the decrease in the pitch angle $\Delta\Theta_L$ for the scattered particles (untrapped particles, for which condition (15) is fulfilled) are comparable for both types of the packet amplitude profile. This indicates that the region of efficient nonlinear interaction of the particle with the wave is small in this case compared with the scale of the amplitude variation in the Gaussian packet. As it should have been expected, the value $\Delta\Theta_L$ can be noticeably greater (in its absolute value) for the trapped particles in the rectangular packet, and the duration of the trapping is longer (the number of zeros in the time dependence of the mismatch is greater).

4. DISCUSSION

As was noted in the Introduction, the main regimes of resonant interaction of a particle with a quasimonochromantic wave packet are the linear regime corresponding to scattering with no systematic variation in the energy and/or pitch angle, the phase bunching regime, where an average variation in the pitch angle, which is determined by the resonance type, occurs along with the scattering, and the regime of particle trapping by the wave field, which is characterized by the drift of the particle in the phase space, with the direction of the drift being determined by the sign of the effective inhomogeneity. In [29], the regime of directed scattering of untrapped particles is also identified, which is determined, in the authors' opinion, by the influence of force bunching (the second term in Eq. (4) for the wave phase).

In the region of parameters considered here and corresponding to the experimental data [19], all three nonlinear regimes specified above are possible. The directed scattering of untrapped particles (strong decrease in the pitch angle) is observed in the range of initial angles $\Theta_{L0}^{\rm NL} \le \Theta_{L0} \le \Theta_{L0}^{\rm un}$, bunching of

untrapped particles (insignificant increase in the pitch angle, which depends weakly on the initial phase) is observed at $\Theta_{L0} \geq \Theta_{L0}^{\mathrm{NL}}$, and particle trapping by the wave field, at $\Theta_{L0} \geq \Theta_{L0}^{\mathrm{tr}} > \Theta_{L0}^{\mathrm{NL}}$. Specific values of $\Theta_{L0}^{\mathrm{NL}}$, $\Theta_{L0}^{\mathrm{un}}$, and $\Theta_{L0}^{\mathrm{tr}}$ (as well as the ratio of the pitch angles $\Theta_{L0}^{\mathrm{un}}$ and $\Theta_{L0}^{\mathrm{tr}}$) depend on the electron energy, the packet amplitude profile, and the packet position.

In [23], where the calculations for the monochromatic wave with a constant amplitude were performed, directed scattering of untrapped particles was not observed. Probably, the presence of this regime under the conditions of our calculations is connected with a higher wave amplitude. Additionally, the finite length of the packet, which limits the zone of the resonance interaction (at high amplitudes), and the frequency drift can be of importance.

Excluding the scattering of untrapped particles, the results that we obtained agree qualitatively with the results of [23], namely, starting at a certain pitch angle $\Theta_{L0}^{\mathrm{NL}}$, the dependences $\Delta\Theta_L(\Psi_0)$ have an extended interval with $\Delta\Theta_L \approx \mathrm{const} > 0$, and the resonance phases of the corresponding particles lie in interval (13), which indicates phase bunching. However, in [23], good qualitative agreement with estimates (12) is also noted. Under the conditions of our calculations, qualitative estimates (12) are either formally inapplicable or yield a significantly overstated value. Primarily, this is connected with a higher wave amplitude. However, as in the case with particle scattering, the finite length of the packet and the frequency drift can also be significant.

Let us discuss the directed scattering of the untrapped particles in greater detail. In numerical calculations in [29], where packets with the amplitude profile being close to the real one were considered, the directed scattering was observed for the particles with a low pitch angle (untrapped particles or particles escaping from the trapping regime). The authors of [29] explained the nonlinear directed scattering of the particles with low pitch angles by compensation for the mismatch Δ due to the second term in Eq. (4) (force bunching), which is proportional to the wave amplitude. The second term is usually neglected in the analytical consideration [32].

To verify this interpretation, Fig. 10 presents time dependences of the left-hand side of Eq. (4) and two terms on the right-hand side along the trajectory of the transit-type particle with a great decrease $\Delta\Theta_L$ in the vicinity of the resonance for the cases shown in Fig. 3 and Fig. 7 (for the scattered particle with the greatest decrease in the pitch angle). For comparison, we also show the results for an arbitrary untrapped particle with a small $\Delta\Theta_L$ (black lines in Fig. 3 and Fig. 7). One can see in the figure that in both cases, for the untrapped particle with a strong decrease in the pitch angle in the vicinity of the resonance the second term on the right-hand side of Eq. (4) is indeed of the same order as the mismatch $-\Delta$. In different realization, the terms can have different signs, both before and after the resonance point (the right and left columns in Fig. 10, respectively), and this trajectory interval corresponds to the efficient decrease in the pitch angle. For particles with a small resulting variation in the pitch angle, the second term is negligibly small even in the vicinity of the resonance, and the curves corresponding to $-\Delta$ and $\mathrm{d}\Psi/\mathrm{d}t$ are almost indistinguishable. However, in this case, the difference between the dependences $\mathrm{d}\Psi/\mathrm{d}t$, which are shown by black and blue lines, is pronounced much stronger for both presented examples, than the difference between the dependences $\mathrm{d}\Psi/\mathrm{d}t$ and $-\Delta$ corresponding to the blue lines. It follows from here that the influence of the force bunching has a quantitative, rather than qualitative character, and the relatively slow change in the mismatch is determined by the particle's stay in the vicinity of the separatrix dividing the trapped and transit-type particles on the phase plane. In this case, the directed scattering is possible also for the particles with significantly higher pitch angles than it follows from the comparison of the first and second terms on the right-hand side of Eq. (4).

The distribution of untrapped particles with a strong decrease in the pitch angle over the resonance phases demonstrates the following (see the right columns in Figs. 3–8). At low pitch angles (those exceeding R^0, i.e. for a weak nonlinearity), a greater fraction of such particles has resonance phases in the vicinity of $7\pi/4$, which corresponds to the maximum decrease in the value $\Delta\Theta_L$ in the linear case. The decrease itself in this case can exceed $|\Delta\Theta_L^{\mathrm{lin}}|$ significantly, which is determined by a long-term stay of the particle in the vicinity of the separatrix (at $R^0 \gtrsim 1$, when the separatrix is absent, i.e., in the vicinity of the inflexion point

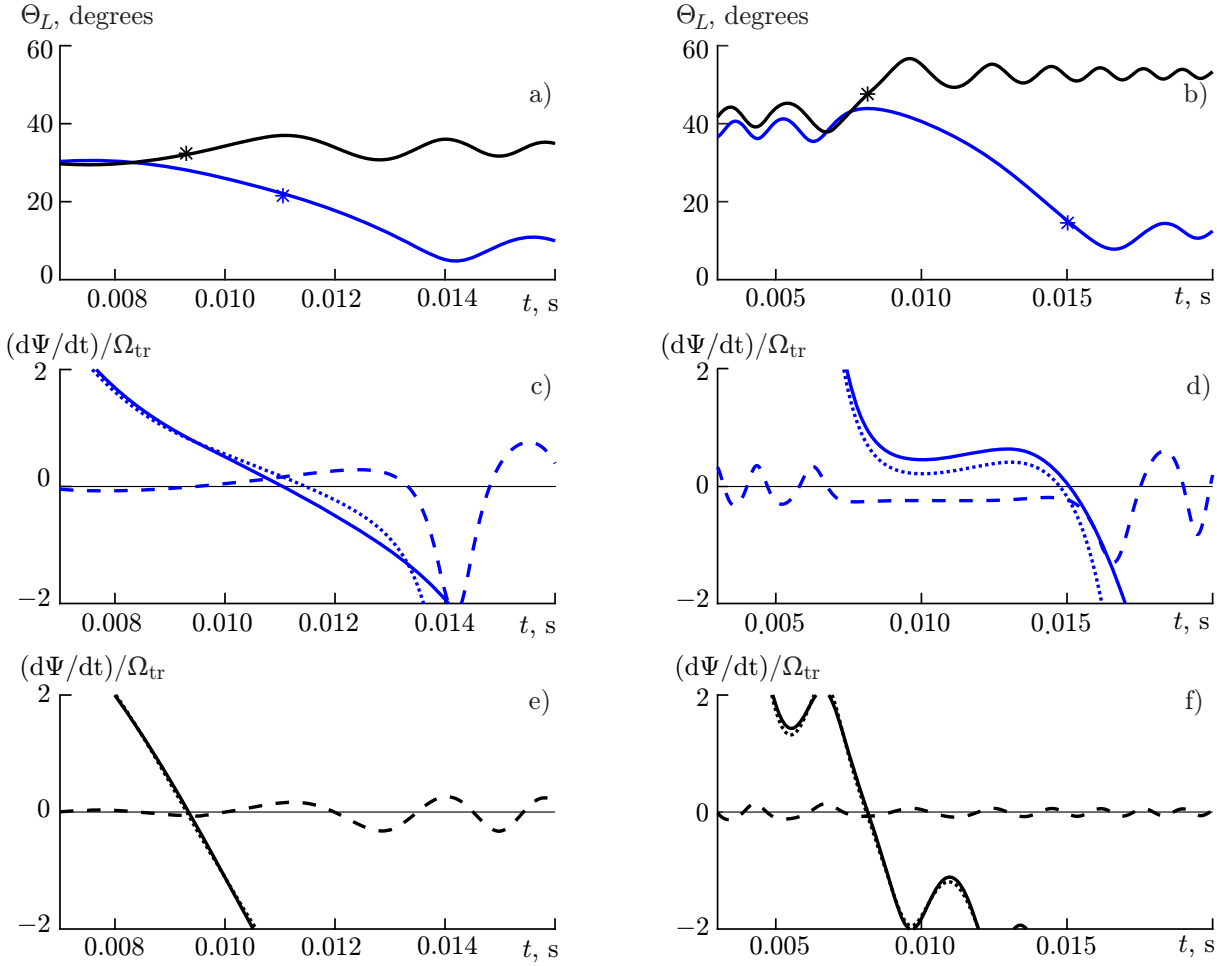

Fig. 10. Calculation results for the untrapped particles with a great variation in the pitch angle (packet 2) for the Gaussian packet (left column, $W_0 = 0.98$ MeV, $\Theta_{L0} = 30°$) and the rectangular packet (right column, $W_0 = 1.15$ MeV, $\Theta_{L0} = 40°$). The asterisks on panels *a* and *b* mark the resonance points. The solid lines in panels *c*–*f* correspond to $-\Delta$ (the first term on the right-hand side of Eq. (4)), the dashed lines correspond to the term proportional to $\cos\Psi$ (the second term on the right-hand side of Eq. (4)), and the dotted lines, to the total derivative $\mathrm{d}\Psi/\mathrm{d}t$.

of the effective potential). At intermediate pitch angles (i.e., smaller than R^0), the scattered particles have resonance phases in the vicinity of Ψ_{turn}, which corresponds to the stay of the particles in the vicinity of the separatrix far from the saddle. It is evident that the noticeable increase in the time of the particle's stay in this region on the phase plane takes place under the conditions of a shallow potential well, i.e., in the case of low probability of the trapping.

Thus, the following can be said about the properties of the directed scattering. At low initial pitch angles, force bunching [29] can yield a small quantitative effect. At the intermediate initial pitch angles, the trajectories corresponding to the directed scattering are transitional between the trajectories of the untrapped and trapped particles. The decrease in or vanishing of the directed scattering at high pitch angles can be connected both with the transition of the scattered particles to the trapped ones (see Fig. 5 and Fig. 6), and with the enhancement of the bunching effect (see Fig. 8).

It has been noted above that the characteristics of the nonlinear interaction are largely determined by the frequency drift. Along with the frequency dependence of the resonance interaction region, which can be regarded as a kinematic effect, the change in the frequency affects strongly the effective-inhomogeneity parameter $\mathcal{R}$, which determines the probability of the trapping and the motion of the trapping region in the

phase space, i.e., the value and sign of the change in the pitch angle (and, in the general case, energy) of the trapped particles. As the parameter $|\mathcal{R}|$ increases, the size of the potential well and, correspondingly, the number of trapped particles decrease, but the rate of variation in the pitch angle and energy of the particles increases (see, e.g., [30, 33]).

In the absence of the frequency drift, the value of the effective-inhomogeneity parameter decreases for the considered type of the interaction (due to the term $-k_{||}v_{||}$ in the mismatch Δ). Correspondingly, for quasimonochromatic wave packets (with no frequency drift), the number of trapped particles increases, but the average change in the pitch angle decreases. This was confirmed by test calculations. The calculation results are omitted for brevity. The directed scattering in the absence of the frequency drift also leads to a generally smaller variation in the pitch angle and, additionally, takes place for a significantly smaller number of particles.

The integral characteristics of the efficiency of interaction of electrons with an ICW package depending on the electron energy and the package properties will be considered in the second part of the work.

5. CONCLUSIONS

Let us summarize the main results obtained here.

The interaction of relativistic electrons with a finite-width packet of ion-cyclotron waves with a frequency drift has been considered. Three nonlinear interaction regimes, which are possible at $R \lesssim 1$, have been studied, specifically, bunching, directed scattering of untrapped particles, and particle trapping by the wave field.

Bunching of untrapped particles is phase grouping of the particles, which results in their crossing the separatrix separating the untrapped particles and the trapped ones in the vicinity of the saddle point. Under the considered conditions, where the parameter of the effective inhomogeneity is $\mathcal{R} < 0$, it leads to a slight increase in the pitch angle by about the same value for a large fraction of the untrapped particles. This regime was described analytically in [31, 32]. Our results agree with this analysis qualitatively. Quantitatively, analytical estimates yield an overstated value of $\Delta\Theta_L^{\mathrm{NL}}$, which may be due to a high wave amplitude under the conditions of our calculations, or with the finite length of the wave packet.

Directed scattering is a strong decrease in the pitch angle of a small fraction of untrapped particles. It was claimed in [29] that it is possible only for low pitch angles and is determined by the influence of the azimuthal component of the Lorentz force (force bunching of particles). Our results show that directed scattering is possible in a noticeable wider range of pitch angles and is determined by a long-term stay of the particle on the phase plane in the region of the separatrix far from the saddle. Force bunching has a quantitative and, moreover, comparatively weak influence on this process. This infuence is noticeable at low initial pitch angles. At intermediate pitch angles, the trajectories corresponding to the directed scattering constitute the transitional region between the trajectories of the untrapped and trapped particles.

Directed scattering and trapping of particles by the wave field at $\mathcal{R} < 0$ can lead to efficient precipitation of electrons into the loss cone, whereas bunching, by contrast, determines an increase in the electron pitch angle. Prevalence of this or that nonlinear effect depends on the inhomogeneity parameter R, as well as on the profile of the packet amplitude.

Integral characteristics of the interaction regimes and efficiency of scattering of electrons into the loss cone depending on their energy, the profile of the packet amplitude, and the position of the packet in space will be presented in the second part of this work.

This work was supported by the Russian Science Foundation (project No. 15–12–20005).

REFERENCES

1. B. J. Anderson and D. C. Hamilton, *J. Geophys. Res.: Space Physics*, **98**, No. A7, 11369 (1993).
2. B. J. Fraser and T. S. Nguyen, *J. Atmosph. Solar-Terr. Phys.*, **63**, 1225 (2001).

3. T. M. Loto'aniu, B. J. Fraser, and C. L. Waters, *J. Geophys. Res.: Space Physics*, **110**, A07214 (2005).
4. M. E. Usanova, I. R. Mann, J. Bortnik, et al., *J. Geophys. Res.: Space Physics*, **117**, No. A10, A10218 (2012).
5. K. Keika, K. Takahashi, A. Y. Ukhorskiy, and Y. Miyoshi, *J. Geophys. Res.: Space Physics*, **118**, No. 7, 4135 (2013).
6. E. N. Ermakova, A. G. Yahnin, T. A. Yahnina, et al., *Radiophys. Quantum Electron.*, **58**, No. 8, 547 (2015).
7. J. Kangas, A. Guglielmi, O. Pokhotelov, *Space Sci. Rev.*, **83**, 435 (1998).
8. A. Demekhov, *J. Atmosph. Solar-Terr. Phys.*, **69**, 1609 (2007).
9. M. J. Engebretson, A. Keiling, K.-H. Fornacon, et al., *Planet. and Space Sci.*, **55**, 829 (2007).
10. M. J. Engebretson, J. L. Posch, A. M. Westerman, et al., *J. Geophys. Res.: Space Physics*, **113**, No. A7, A07206 (2008).
11. J. S. Pickett, B. Grison, Y. Omura, et al., *Geophys. Res. Lett.*, **37**, L09104 (2010).
12. P. A. Bespalov and V. Yu. Trakhtengerts, *Alfvén Masers* [in Russian], Inst. Appl. Phys., Gorky (1986).
13. O. Santolik, D. Gurnett, J. Pickett, et al., *J. Geophys. Res.*, **108**, No. A7, 1278 (2003).
14. V. Y. Trakhtengerts, *J. Geophys. Res.*, **100**, No. 9, 17205 (1995).
15. V. Trakhtengerts and A. Demekhov, *J. Atmosph. Solar-Terr. Phys.*, **69**, 1651 (2007).
16. Y. Omura, J. Pickett, B. Grison, et al., *J. Geophys. Res.: Space Physics*, **115**, A07234 (2010).
17. M. Shoji, Y. Omura, B. Grison, et al., *Geophys. Res. Lett.*, **38**, No. 17, L17102 (2011).
18. K. Mursula, *J. Atmosph. Solar-Terr. Physics*, **69**, 1623 (2007).
19. M. J. Engebretson, J. L. Posch, J. R. Wygant, et al., *J. Geophys. Res.: Space Physics*, **120**, 5465 (2015).
20. R. M. Thorne and C. F. Kennel, *J. Geophys. Res.*, **76**, No. 19, 4446 (1971).
21. D. Summers and R. M. Thorne, *J. Geophys. Res.: Space Physics*, **108**, No. A4, 1143 (2003).
22. V. K. Jordanova, J. Albert, and Y. Miyoshi, *J. Geophys. Res.: Space Physics*, **113**, No. A3, A00A10 (2008).
23. J. M. Albert and J. Bortnik, *Geophys. Res. Lett.*, **36**, No. 12, L12110 (2009).
24. K. Liu, D. Winske, S. P. Gary, and G. D. Reeves, *J. Geophys. Res.: Space Physics*, **117**, No. A6, A06218 (2012).
25. G. Khazanov, D. Sibeck, A. Tel'nikhin, and T. Kronberg, *Phys. Plasmas*, **21**, No. 8, 082901 (2014).
26. A. V. Artemyev, D. Mourenas, O. V. Agapitov, et al., *Phys. Plasmas*, **22**, No. 8, 082901 (2015).
27. Y. Omura and Q. Zhao, *J. Geophys. Res.: Space Physics*, **117**, No. A8, A08227 (2012).
28. Y. Omura and Q. Zhao, *J. Geophys. Res.: Space Physics*, **118**, No. 8, 5008 (2013).
29. Y. Kubota and Y. Omura, *J. Geophys. Res.: Space Physics*, **122**, No. 1, 293 (2017).
30. V. I. Karpman, Y. N. Istomin, and D. R. Shklyar, *Plasma Phys.*, **16**, No. 8, 685 (1974).
31. J. M. Albert, *Phys. Fluids B*, **5**, 2744 (1993).
32. J. M. Albert, *J. Geophys. Res.*, **105**, 21191 (2000).
33. A. G. Demekhov, V. Yu. Trakhtengerts, M. Rycroft, and D. Nunn, *Geomagn. Aeron.*, **46**, No. 6, 711 (2006).
34. V. Y. Trakhtengerts, M. J. Rycroft, D. Nunn, and A. G. Demekhov, *J. Geophys. Res.: Space Physics*, **108**, 1138 (2003).
35. D. R. Shklyar, *Ann. Geophys.*, **29**, 1179 (2011).